Hindawi Publishing Corporation
Mathematical Problems in Engineering
Volume 2012, Article ID 720849, 15 pages
doi:10.1155/2012/720849

Research Article

Study on Apparent Kinetic Prediction Model of the Smelting Reduction Based on the Time-Series

Guo-feng Fan,[1] Shan Qing,[1] Hua Wang,[1] Zhe Shi,[1] Wei-Chiang Hong,[2] and Lin Dai[3]

[1] *Engineering Research Center of Metallurgical Energy Conservation and Emission Reduction, Ministry of Education, Kunming University of Science and Technology, Kunming, Yunnan 650093, China*
[2] *Department of Information Management, Oriental Institute of Technology, 58, Sec. 2, Sichuan Roa., Panchiao, Taipei 200, Taiwan*
[3] *Faculty of Science, Kunming University of Science and Technology, Kunming, Yunnan 650093, China*

Correspondence should be addressed to Hua Wang, wanghuaheat@hotmail.com

Received 29 December 2011; Revised 2 March 2012; Accepted 8 March 2012

Academic Editor: Yuri Vladimirovich Mikhlin

A series of direct smelting reduction experiment has been carried out with high phosphorous iron ore of the different bases by thermogravimetric analyzer. The derivative thermogravimetric (DTG) data have been obtained from the experiments. One-step forward local weighted linear (LWL) method , one of the most suitable ways of predicting chaotic time-series methods which focus on the errors, is used to predict DTG. In the meanwhile, empirical mode decomposition-autoregressive (EMD-AR), a data mining technique in signal processing, is also used to predict DTG. The results show that (1) EMD-AR(4) is the most appropriate and its error is smaller than the former; (2) root mean square error (RMSE) has decreased about two-thirds; (3) standardized root mean square error (NMSE) has decreased in an order of magnitude. Finally in this paper, EMD-AR method has been improved by golden section weighting; its error would be smaller than before. Therefore, the improved EMD-AR model is a promising alternative for apparent reaction rate (DTG). The analytical results have been an important reference in the field of industrial control.

1. Introduction

The complexities in smelting reduction process of iron and steel come from the interaction between the fluid dynamics and chemical kinetics mechanisms. The research direction has changed to how to establish hybrid kinetic model by combining fluid dynamics equations with chemical kinetics algebraic equations and taking factors at the level of microchemical reactions into consideration. Some macrokinetic parameters should be modeled, such as the volume of wind, differential pressure, and feed rate (obtained by dynamic and real-time detection in the process). However, micro-kinetic parameters in chemical reaction process cannot be got by detection and identification online. The apparent reaction rate changes

with the chemical reaction and fluid. In addition, the significance of its kinetic analysis is pretty obvious. Thus, the majority of research focuses on mathematical and physical model based on kinetics [1–4]. There are many uncertain factors affecting the apparent reaction rate. Moreover, a great difference exists between the physical model of smelting reduction and the unreacted-core model in the blast furnace. So its calculation model would not be accurate enough, even nonignorable errors exist [5]. One advantage of time-series analysis methods is to infer the future value from the historical value without considering other factors. Time-series analysis methods are very convenient and accurate to study the evolution of apparent reaction rate. In this paper, time-series analysis methods are used to study the prediction model on the DTG data (apparent reaction rate) obtained by thermo gravimetric technique. It can be seen that the model has expressed the dynamic process of smelting reduction and has got high hit rate under uncertainty. Finally, the predicting method has been improved effectively.

The rest of the paper is organized as follows. In Section 2, the appropriate predicting method is employed to analyze the features of derivative thermo gravimetric data. The one-step forward local weighted linear method and its analysis and discussion of the experimental data are shown in Section 3. The EMD method and AR model for analyzing experimental data will be presented in Section 4; in the meanwhile, some improvement of the EMD-AR model is also provided. Finally, a brief summary is discussed in Section 5.

2. Features Analysis of Derivative Thermogravimetric Data

First, the features of DTG are analyzed. Correlation dimension, an important evidence to establish the existence of chaotic continuous systems, is calculated with the reconstruction map of the fractal dimension. For the truly random signals, the correlation dimension graph will look like a 45-degree straight line. It is indicating that no matter how you embed the noise, it will evenly fill that space. Chaotic (or periodic) signals have a distinct spatial structure, and their correlation dimension will saturate as some point while embedding dimension is increased.

The correlation dimension reaches saturation by calculating the correlation dimension of DTG data, as shown in Figure 1. It is shown that the nonlinear chaotic characteristics exist in the system.

In VRA (visual recurrence analysis), we can construct such a model from a range of classes, such as nearest neighbor, locally constant, kernel regression, locally linear, locally weighted linear, radial basis models, and support vector regression [6–9]. Then, the appropriate predicting method is selected. In general, the methods of predicting chaotic time-series include multistep and one-step. One-step is better than multistep for the errors curve of DTG. Locally weighted linear method, one of the one-step methods, is superior to other methods for the errors' curve of DTG.

3. Prediction Analyses of One-Step Forward Locally Weighted Linear Method

3.1. Locally Weighted Linear (LWL) Method

With a given time-series $\{x_1, x_2, x_3, \ldots x_n\}$ composed of n observations, multistep-ahead prediction consists of predicting $\{x_{n+1}, x_{n+2}, x_{n+3}, \ldots x_{n+h}\}$. The h next values of the time-series, where $h > 1$, are the so-called prediction horizon [10, 11].

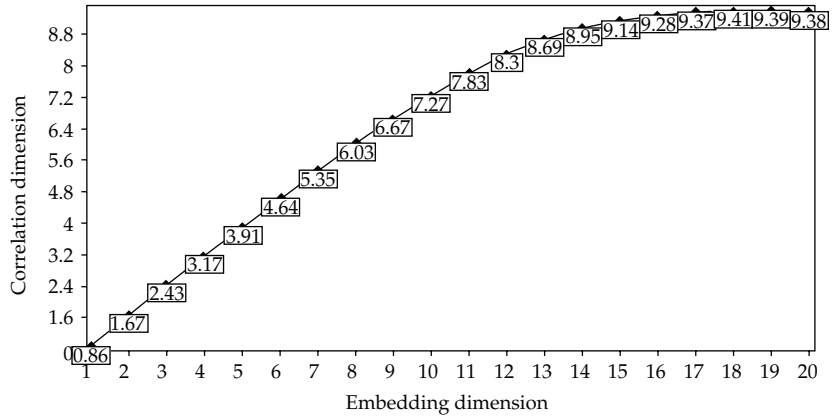

Figure 1: Evolution diagram of correlation dimension.

One-step estimate is generated by

$$x_{n+1} = f\left(x_n, x_{n-t}, x_{n-2t}, \ldots x_{n-(d-1)t}\right), \tag{3.1}$$

where d is the embedding dimension and t is time delay.

Suppose $X = (x_n, x_{n-t}, x_{n-2t}, \ldots x_{n-(d-1)t})$ and $X_i = (x_i, x_{i-t}, x_{i-2t}, \ldots x_{i-(d-1)t})$, $1 \le i \le k$, where k is neighborhoods.

The weight of X_i is defined by

$$P_i = \frac{K(d_i)}{\sum_{i=1}^{k} K(d_i)}, \tag{3.2}$$

where $K(\cdot)$ is essentially a weighting function used to assign the contribution of each neighbor to the prediction in locally weighted linear predictor and d_i is the distance between X and X_i. The Gaussian kernel function is to be used here, which is calculated in the following:

$$K(\cdot) = \exp -\left(\frac{\text{distance}}{k}\right)^2, \tag{3.3}$$

where distance is the Euclidean distance.

The locally weighted linear methods can be expressed in

$$\begin{bmatrix} X_2 \\ X_3 \\ \cdots \\ X_{h+1} \end{bmatrix} = \begin{bmatrix} e & X_1 \\ e & X_2 \\ \cdots & \cdots \\ e & X_h \end{bmatrix} \begin{bmatrix} a \\ b \end{bmatrix}, \tag{3.4}$$

where $e = \begin{bmatrix} 1 \\ 1 \\ \ldots \\ 1 \end{bmatrix}_d$.

The situation that the embedding dimension is one ($m = 1$) was discussed; others ($m > 1$) are similar:

$$\begin{bmatrix} x_2 \\ x_3 \\ \cdots \\ x_{h+1} \end{bmatrix}_d = \begin{bmatrix} e & x_1 \\ e & x_2 \\ \cdots & \cdots \\ e & x_h \end{bmatrix} \begin{bmatrix} a \\ b \end{bmatrix}. \tag{3.5}$$

The weighted least squares method is applied to (3.5), which can be demonstrated as

$$\sum_{i=1}^{h} P_i (x_{i+1} - a - bx_i)^2 = \min. \tag{3.6}$$

Then partial derivatives of a or b are as follows:

$$\begin{aligned} \sum_{i=1}^{h} P_i (x_{i+1} - a - bx_i) &= 0, \\ \sum_{i=1}^{h} P_i (x_{i+1} - a - bx_i) x_i &= 0. \end{aligned} \tag{3.7}$$

Solutions are expressed in

$$\begin{aligned} a &= \sum_{i=1}^{h} P_i x_{i+1} - \frac{\left(\sum_{i=1}^{h} P_i x_i\right)\left(\sum_{i=1}^{h} P_i x_{i+1}\right) - \left(\sum_{i=1}^{h} P_i x_{i+1} x_i\right)}{\left(\sum_{i=1}^{h} P_i x_i\right)^2 - \left(\sum_{i=1}^{h} P_i {x_i}^2\right)} \times \left(\sum_{i=1}^{h} P_i x_i\right), \\ b &= \frac{\left(\sum_{i=1}^{h} P_i x_i\right)\left(\sum_{i=1}^{h} P_i x_{i+1}\right) - \left(\sum_{i=1}^{h} P_i x_{i+1} x_i\right)}{\left(\sum_{i=1}^{h} P_i x_i\right)^2 - \left(\sum_{i=1}^{h} P_i {x_i}^2\right)}. \end{aligned} \tag{3.8}$$

Taking a, b into $x_{n+1} = a + bx_n$, then, the predicted value was got.

$$\begin{aligned} x_{n+1} = \sum_{i=1}^{h} P_i x_{i+1} &- \frac{\left(\sum_{i=1}^{h} P_i x_i\right)\left(\sum_{i=1}^{h} P_i x_{i+1}\right) - \left(\sum_{i=1}^{h} P_i x_{i+1} x_i\right)}{\left(\sum_{i=1}^{h} P_i x_i\right)^2 - \left(\sum_{i=1}^{h} P_i {x_i}^2\right)} \times \left(\sum_{i=1}^{h} P_i x_i\right) \\ &+ \frac{\left(\sum_{i=1}^{h} P_i x_i\right)\left(\sum_{i=1}^{h} P_i x_{i+1}\right) - \left(\sum_{i=1}^{h} P_i x_{i+1} x_i\right)}{\left(\sum_{i=1}^{h} P_i x_i\right)^2 - \left(\sum_{i=1}^{h} P_i {x_i}^2\right)} \times x_n. \end{aligned} \tag{3.9}$$

The calculated performance is otherwise known as the root mean square error (RMSE) and the normalized mean squared error (NMSE). NMSE increased the role of large-value

Table 1: Compositions of each type of materials required.

Bases (R)	0.8	1.1	1.4	1.7	2.0
Mineral content (mg)	7.48	6.85	6.82	6.53	6.37
Coal content (mg)	1.40	1.17	1.16	1.11	1.09
Calcium oxide content (mg)	1.12	1.98	2.02	2.36	2.54

Table 2: Errors analysis.

Bases (R)	One-step LWL	
	RMSE	NMSE
0.8	0.1099	0.8771
1.1	0.1047	0.9404
1.4	0.1059	0.9841
1.7	0.1073	0.9704
2.0	0.1196	0.9031

errors in the indicators, thereby improved the sensitivity of this indicator. Equations (3.10) and (3.11) are using one-step prediction:

$$\mathrm{RMSE} = \sqrt{\frac{\sum_{i=1}^{n} (p_i - a_i)^2}{n}}, \tag{3.10}$$

$$\mathrm{NMSE} = \max\left\{ \frac{\sum_{i=1}^{n} (p_i - a_i)^2}{\sum_{i=1}^{n} (\mathrm{mean} - a_i)^2}, \frac{\sum_{i=1}^{n} (p_i - a_i)^2}{\sum_{i=1}^{\mathrm{i}} (a_{i-1} - a_i)^2} \right\}, \tag{3.11}$$

where p_i is the predictive value and a_i is the real value.

Based on (3.11), the smaller NMSE is from the predicted values and actual values. The predictions are quite accurate, and the NMSE for the prediction of 200 points is only 0.8771. That means our predictive model explains about 99.123% of the variance in the series.

3.2. Results and Discussion

Derivative thermogravimetric data of the Huimin ore reflect the change of the apparent reaction rate in the smelting reduction process. Experiment extent is confirmed with bases 0.8, 1.1, 1.4, 1.7, 2.0; respectively, the compositions of each type of materials required are shown in Table 1.

The TGA experiment equipment is produced by Netzsch, modeling as STA 449 F3. It is protected with nitrogen gas flowing at 50 mL/min. And argon, acting as purge gas, flows at the rate of 10 mL/min. There are 200 points around 1400°C predicted. The performances of their prediction charts using one-step forward locally weighted linear method are shown in Figure 2.

From Figure 2, the prediction is well matched, especially in the trend of rise or decline. It is shown that RMSE remains at about 0.1, and the error is small and stable in Table 2; in the meanwhile, NMSE is maintained at about 0.9, which explains more than 99% of the variance.

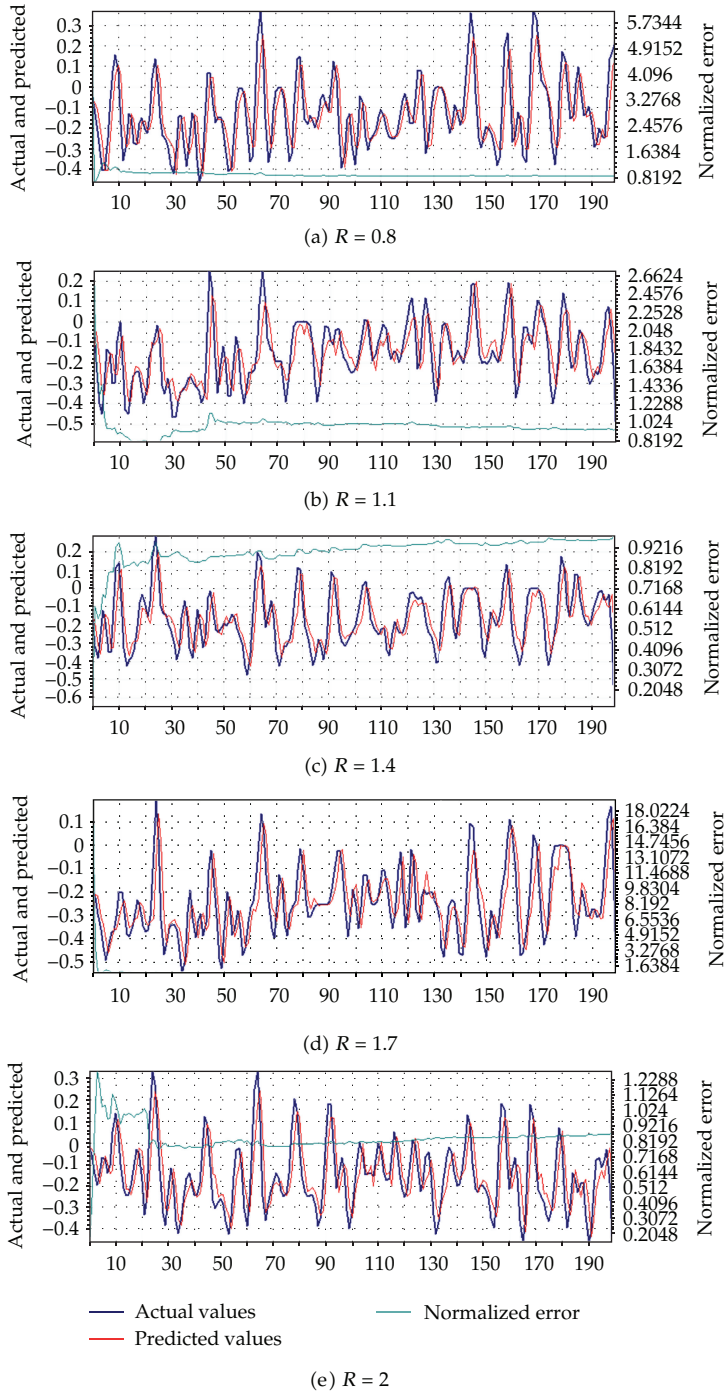

(a) $R = 0.8$

(b) $R = 1.1$

(c) $R = 1.4$

(d) $R = 1.7$

(e) $R = 2$

Figure 2: Prediction effect for different values of R.

4. Prediction Analysis of Derivative Thermogravimetric Data of the EMD-AR Method

Empirical mode decomposition (EMD) has been successfully applied to many fields, such as communication, society, economy, engineering, and achieved good effects [12–19]. The AR model forecasting methods is intended to apply to the system of smelting reduction.

4.1. Empirical Mode Decomposition

EMD method is developed from the simple assumption that any signal consists of different simple intrinsic modes of oscillations. Each linear or nonlinear mode will have the same number of extreme and zero crossings. There is only one extreme between successive zero-crossings. Each mode should be independent of the others. In this way, each signal could be decomposed into a number of intrinsic mode functions (IMFs), each of which must satisfy the following definitions [15].

(a) In the whole data set, the number of extreme and the number of zero-crossings must either equal or differ from each other at most by one.

(b) At any point, the mean value of the envelope defined by local maxima and the envelope defined by the local minima is zero.

An IMF represents a simple oscillatory mode compared with the simple harmonic function.

With the definition, any signal $x(t)$ can be decomposed as follows.

(1) Identify all local extremes, and then connect all the local maxima by a cubic spline line as the upper envelope.

(2) Repeat the procedure for the local minima to produce the lower envelope. The upper and lower envelopes should cover all the data among them.

(3) The mean of upper and low envelope value is designated as m_1, and the difference between the signal $x(t)$ and m_1 is the first component, h_1; that is,

$$h_1 = x(t) - m_1. \tag{4.1}$$

Generally speaking, h_1 will not necessarily meet the requirements of the IMF, because h_1 is not a standard IMF. It needs to be selected for k times until the mean envelope tends to zero. Then the first intrinsic mode function c_1 is denoted, which stands for the most high-frequency component of the original data sequence. At this point, the data could be represented as

$$h_{1k} = h_{1(k-1)} - m_{1k}, \tag{4.2}$$

where h_{1k} is the datum after k times' siftings. $h_{1(k-1)}$ stands for the datum after $k-1$ times' sifting. Standard deviation (SD) is used to determine whether the results of each filter component meet the IMF or not. SD is defined as

$$\mathrm{SD} = \sum_{k=1}^{T} \frac{\left|h_{1(k-1)}(t) - h_{1k}(t)\right|^2}{h_{1(k-1)}^2(t)}, \tag{4.3}$$

where T is the length of the data.

The value of standard deviation SD is limited in the range of 0.2 to 0.3, which means that when $0.2 < \mathrm{SD} < 0.3$, the decomposition process can be finished. The physical considerations of this standard are the following: it is necessary to not only ensure $h_k(t)$ to meet the IMF requirements but also control the decomposition times. So in this way the IMF components could retain amplitude modulation information in the original signal.

(4) When h_{1k} has met the basic requirements of SD on the condition of $c_1 = h_{1k}$, the signal $x(t)$ of the first IMF component c_1 would be gotten and a new series r_1 could be achieved after deleting the high-frequency components. That is to say

$$r_1 = x(t) - c_1. \tag{4.4}$$

The new sequence is treated as the original data, and repeat the above (3.1)–(3.3) processes. Then the second intrinsic mode function c_2 could be got.

(5) Repeat (3.1)–(3.4) until r_n will no longer be decomposed into the IMF. The sequence r_n is called the remainder of the original data $x(t)$. r_n is a monotonic sequence, indicating the overall trend of the raw data $x(t)$ or mean, which is usually referred as the so-called trend items. It is of clear physical significance.

The process is expressed as follows

$$r_1 = x(t) - c_1, r_2 = r_1 - c_2, \ldots, r_n = r_{n-1} - c_n. \tag{4.5}$$

Then,

$$x(t) = \sum_{i=1}^{n} c_i + r_n. \tag{4.6}$$

The original data can be expressed as the IMF component and remainder.

The rate trend characterized by five kinds of base after EMD decomposition is shown in Figure 3.

Seen from Figure 3, the experimental data are divided into 13 groups. The last group is a trend term and parabolic curve, indicating there is an inner maximum of the apparent reaction rate existing in the unsteady-state process. And the temperature ranges from 600 to 800°C; when the temperature falls in this range, various crystalline phases of iron oxides change, but the mass will not change much [20].

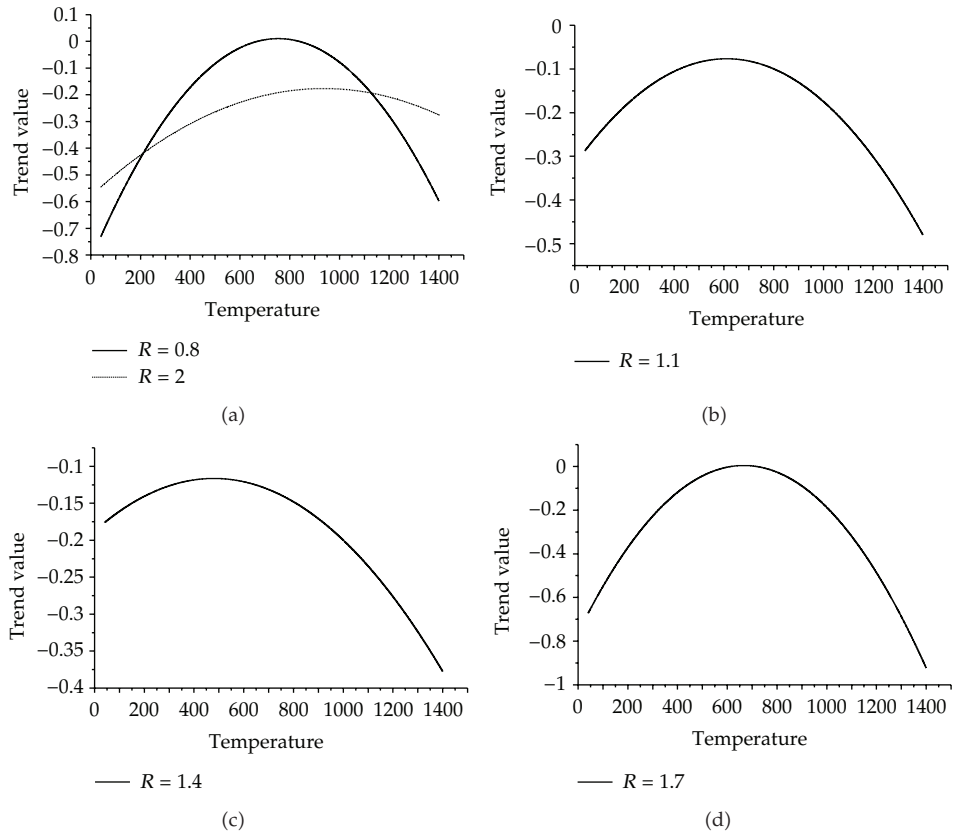

Figure 3: EMD trend line.

4.2. AR Model

Consider

$$X_t = \sum_{j=1}^{p} a_j X_{t-j} + \varepsilon_t, \quad t \in Z. \tag{4.7}$$

Equation (4.7) is a p step autoregressive model, referring as $AR(p)$ model [21]. Stationary time-series $\{X_t\}$ that meets the model $AR(p)$ is called the $AR(p)$ sequence. That $a = (a_1, a_2, \ldots, a_p)^T$ is named as the regression coefficients of the $AR(p)$ model.

4.3. Modified EMD-AR Method

Huimin ore was analyzed with different base at sampling points of 8144, after the decomposition of EMD, the data can be divided into 13 groups, and the last group is a trend term.

Firstly, each component is tried out through the ADF stationary test, as can be seen from Table 3; 1%, 5%, 10% of the values are greater than the level of ADF critical value, which is no unit root. So it can be said to meet the stationary time-series. From Table 4, according to

Table 3: ADF test table.

		t-Statistic	Prob.*
Augmented Dickey-Fuller test statistic		−32.84661	0.0000
Test critical values	1% level	−3.430977	
	5% level	−2.861702	
	10% level	−2.566898	

*MacKinnon 1996 [23] one-sided *P* values.
Augmented Dickey-Fuller test equation.
Dependent variable: D(SER01).
Date: 06/07/11 Time: 16: 10.
Sample (adjusted): 10 8144.
Included observations: 8135 after adjustments.

the geometric decay of the correlation coefficient and partial correlation coefficients fourth-order truncation, it can be regarded as AR (3.4) model. After the analyses of 13 groups, the majority are positioned in AR (3.4). For simplicity, AR (3.4) model should be taken into account.

Then with the previous 7944 data points, each group of data is predicted to 8144 in the method of AR (3.4) model.

Calculation results are represented in

$$x_{n+1} = \sum_{i=2}^{13} \sum_{j=0}^{3} a_{n-j,i} \times x_{n-j,i}, \tag{4.8}$$

where $x_{n-j,i}$ is the autoregressive variable of the ith component. $a_{n-j,i}$ is the corresponding self-group regression coefficients.

Equation (4.9) is revised by the golden section weighting:

$$\overline{x_{n+1}} = 0.618x_{n+1} + 0.382x_n. \tag{4.9}$$

4.4. Analysis and Comparison of Experimental Results

The results calculated by using MATLAB programming are shown in Figure 4.

As can be seen from Figure 4, the trend match is quite well. The overall hit rate is also high, reaching a basic agreement. In Tables 3 and 4, the steadiness can be determined by the decay of autocorrelation and 4 steps truncated of partial autocorrelation, so the fourth-step autoregressive model is taken into account. The chaotic time-series are generally non-stationary, even after repeated differential data cannot be stationary. It is shown that the EMD can compensate the deficiency of nonsteadiness. Prediction performance is poorer when adding white noise disturbance than those without noise, and the deterministic signal is comparatively evident. The model of golden weighted correction is better. The result of error analysis is shown in Table 5.

Based on Table 5, RMSE of EMD-AR method has decreased about two-thirds than the local linear weighting method. NMSE decreased in an order of magnitude. The improved EMD-AR error is smaller. The average error (AE) is also very small, especially minimum errors of $R = 1.1$ and 1.4, where reduction effort was better [22].

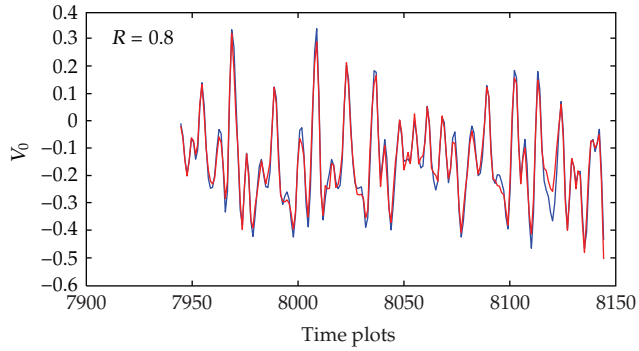

(a) $R = 0.8$

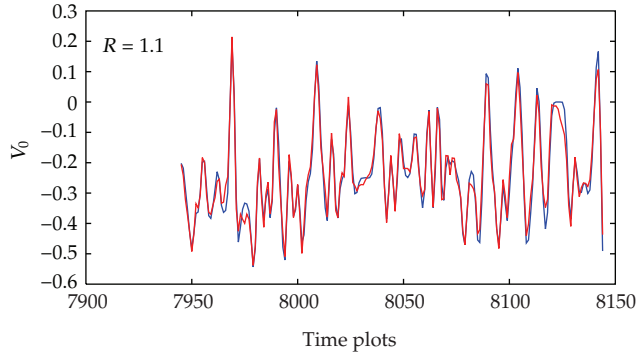

(b) $R = 1.1$

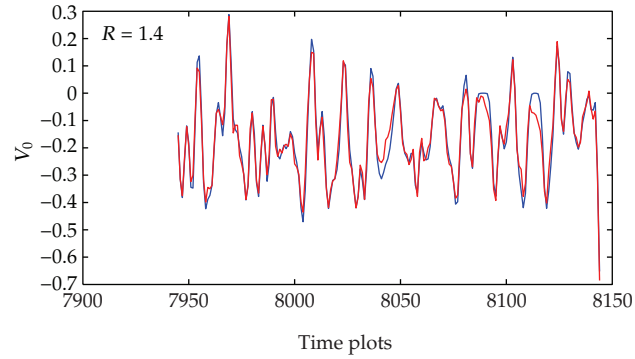

(c) $R = 1.4$

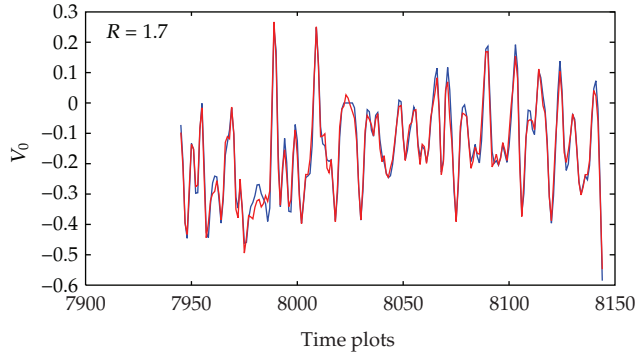

(d) $R = 1.7$

Figure 4: Continued.

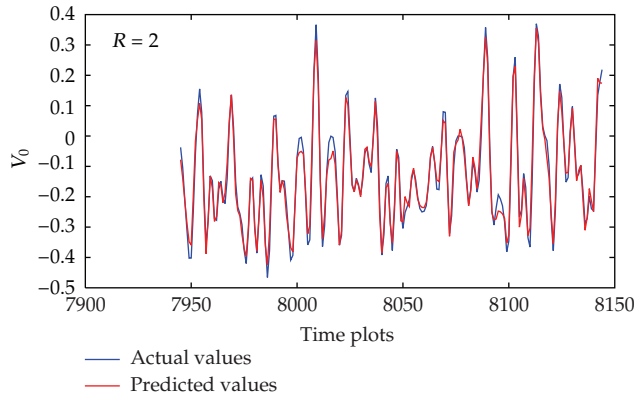

(e) $R = 2.0$

Figure 4: EMD-AR prediction effects.

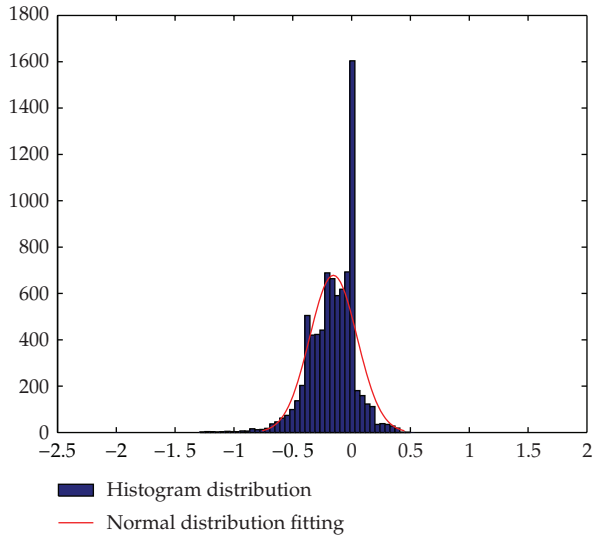

Figure 5: Characteristic of normal distribution for DTG data.

In Figure 5, it is obviously shown the characteristic of the normal distribution for DTG data, which reflect the ergodicity of the apparent reaction rate in the smelting process; Figure 6 further clearly demonstrates the statistical laws of DTG, there exists the pair of "∞" curves (including internal ∞ curve and external ∞ curve, resp.), and many scattered points distribute around the curves. So it can be concluded that it belongs to the random discrete dynamic system, and it will be the breakthrough in the curve equation research.

5. Conclusion

(1) As can be seen, the predicted value was identical with the true value of the DTG using one-step forward locally weighted linear prediction method in a high degree,

Table 4: lists autocorrelation and partial autocorrelation.

Autocorrelation	Partial correlation		AC	PAC	*Q*-Stat	Prob.
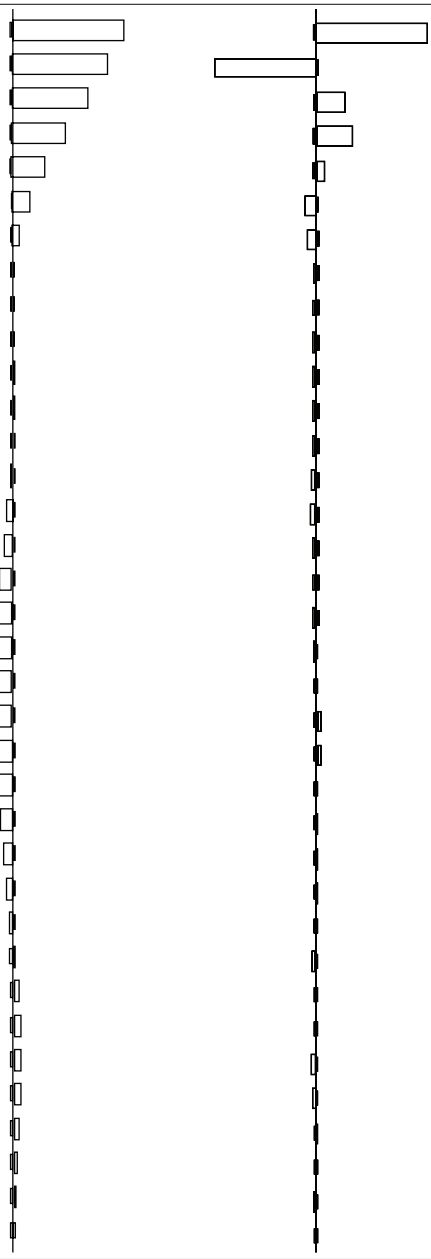		1	0.952	0.952	7384.9	0.0000
		2	0.825	−0.866	12936.	0.0000
		3	0.648	0.253	16355.	0.0000
		4	0.455	0.317	18040.	0.0000
		5	0.279	0.066	18673.	0.0000
		6	0.142	−0.086	18836.	0.0000
		7	0.052	−0.075	18858.	0.0000
		8	0.008	−0.024	18859.	0.0000
		9	−0.003	−0.004	18859.	0.0000
		10	0.003	−0.014	18859.	0.0000
		11	0.013	−0.022	18861.	0.0000
		12	0.016	−0.021	18863.	0.0000
		13	0.007	−0.021	18863.	0.0000
		14	−0.014	−0.034	18865.	0.0000
		15	−0.046	−0.034	18882.	0.0000
		16	−0.081	−0.011	18935.	0.0000
		17	−0.115	−0.007	19042.	0.0000
		18	−0.142	−0.019	19208.	0.0000
		19	−0.162	−0.020	19421.	0.0000
		20	−0.171	0.007	19659.	0.0000
		21	−0.170	0.032	19895.	0.0000
		22	−0.159	0.025	20100.	0.0000
		23	−0.139	0.002	20258.	0.0000
		24	−0.112	0.014	20360.	0.0000
		25	−0.080	0.024	20411.	0.0000
		26	−0.044	0.013	20428.	0.0000
		27	−0.009	0.004	20428.	0.0000
		28	0.022	−0.026	20432.	0.0000
		29	0.048	−0.005	20451.	0.0000
		30	0.064	0.002	20484.	0.0000
		31	0.069	−0.026	20523.	0.0000
		32	0.065	−0.011	20557.	0.0000
		33	0.052	0.013	20579.	0.0000
		34	0.034	−0.005	20589.	0.0000
		35	0.015	−0.018	20591.	0.0000
		36	−0.002	−0.003	20591.	0.0000

which shows that the method is better; this can also be seen by the errors' data itself. The evolution model of the apparent rate is expressed much more clearly.

(2) EMD-AR (3.4) steps have been derived from the data stationary test analysis and autocorrelation and partial correlation coefficient. It is shown that the RMSE of the EMD-AR method has decreased two-thirds than local linear weighting method;

Table 5: Error analysis.

Base (R)	RMSE			NMSE			AE
	One-step LWL	EMD-AR	Improved EMD-AR	One-step LWL	EMD-AR	Improved EMD-AR	Improved EMD-AR
0.8	0.1099	0.0417	0.0306	0.8771	0.0751	0.0679	−0.0017
1.1	0.1047	0.0312	0.0289	0.9404	0.0812	0.0778	−7.53E (−5)
1.4	0.1059	0.0389	0.0326	0.9841	0.0956	0.0935	−6.31E (−4)
1.7	0.1073	0.0527	0.0266	0.9704	0.0678	0.0596	0.0024
2.0	0.1196	0.0297	0.0278	0.9031	0.0534	0.0489	0.0016

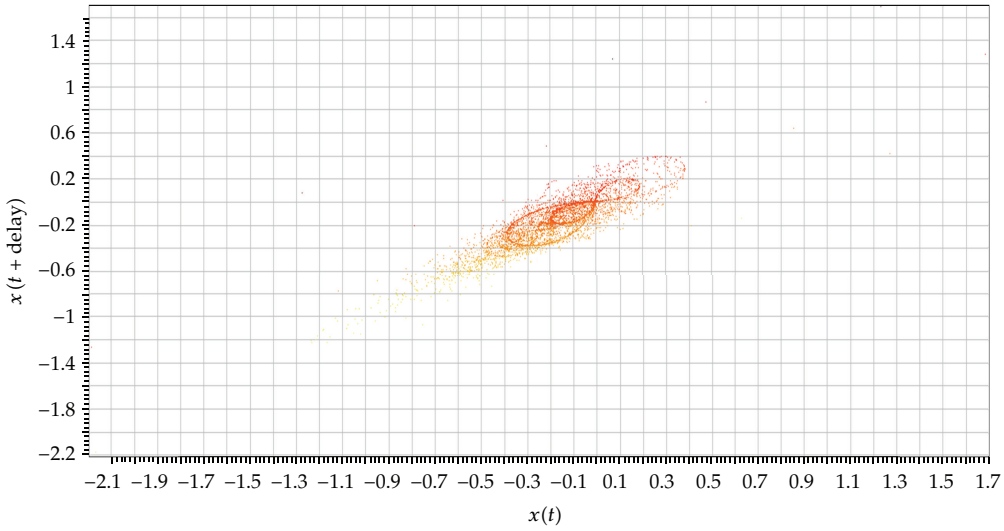

Figure 6: State space chart of DTG ($m = 2$, $\tau = 1$).

NMSE decreased in an order of magnitude. Error of using improved EMD-AR method is smaller; the average error (AE) is also very small, especially minimum errors of $R = 1.1$ and 1.4 where reduction effect is better. It is shown that golden weighted correction to EMD-AR method is effective.

(3) DTG trend item is parabolic curve, indicating there is an inner maximum of the apparent reaction rate existing in the unsteady-state process. And the temperature ranges from 600 to 800°C; when the temperature falls in this range, various crystalline phases of iron oxides changes, but the mass will not change much.

Acknowledgments

This work was supported by National Natural Science Foundation of China under Contract (no. 51064015), the Yunnan Provincial Foundation Key project under Contract (no. ZD2010001), and the National Science Council of Taiwan (NSC 100-2628-H-161-001-MY4), to which the authors are greatly obliged.

References

[1] D. P. Tao, "The kinetic models of chemical reaction of fluids on rough surfaces," *Acta Metallurgica Sinica*, vol. 37, no. 10, pp. 1073–1078, 2001.

[2] W. Ni, M. S. Ma, Y. L. Wang, Z. J. Wang, and F. M. Liu, "Thermodynamic and kinetic in recovery of iron from nickel residue," *Journal of Beijing University of Science and Technology*, vol. 31, no. 2, pp. 163–168, 2009.

[3] Y. Yang, B. Song, S. Yang, Y. Wen, and W. He, "Kinetics of vanadium smelting reduction in a CaO-SiO_2-Al_2O_3 -MgO-V_2O_5 slag system," *Journal of University of Science and Technology Beijing*, vol. 28, no. 12, pp. 1115–1120, 2006.

[4] K. Piotrowski, K. Mondal, H. Lorethova, L. Stonawski, T. Szymański, and T. Wiltowski, "Effect of gas composition on the kinetics of iron oxide reduction in a hydrogen production process," *International Journal of Hydrogen Energy*, vol. 30, no. 15, pp. 1543–1554, 2005.

[5] X. Y. Ma, M. F. Jiang, and D. Wang, "Kinetics and model of reaction process of iron ore-coal pellet," *Journal of Northeastern University*, vol. 23, no. 5, pp. 440–443, 2002.

[6] W. C. Hong, Y. C. Dong, C. Y. Lai, L. Y. Chen, and S. Y. Wei, "SVR with hybrid chaotic immune algorithm for seasonal load demand forecasting," *Energies*, vol. 4, no. 6, pp. 960–977, 2011.

[7] W. C. Hong, "Hybrid evolutionary algorithms in a SVR-based electric load forecasting model," *International Journal of Electrical Power and Energy Systems*, vol. 31, no. 7-8, pp. 409–417, 2009.

[8] P. F. Pai and W. C. Hong, "A recurrent support vector regression model in rainfall forecasting," *Hydrological Processes*, vol. 21, no. 6, pp. 819–827, 2007.

[9] P. F. Pai, C. S. Lin, W. C. Hong, and C. T. Chen, "A hybrid support vector machine regression for exchange rate prediction," *International Journal of Information and Management Sciences*, vol. 17, no. 2, pp. 19–32, 2006.

[10] H. Y. Wu, *Time Series Analysis and Synthesis*, Wuhan University Press, Wuhan, China, 2002.

[11] Q. Meng and Y. Peng, "A new local linear prediction model for chaotic time series," *Physics Letters A*, vol. 370, no. 5-6, pp. 465–470, 2007.

[12] J. X. Xie, C. T. Cheng, G. H. Zhou, and Y. M. Sun, "New direct multi-step ahead prediction model based on EMD and chaos analysis," *Acta Automatica Sinica*, vol. 34, no. 6, pp. 684–689, 2008.

[13] W. Guan and G. W. Xie, "Regression and time series in the application of power load forecasting," *Modern Enterks Culture*, vol. 3, pp. 152–153, 2008.

[14] E. Norden, M. L. Huang, and C. Wu, "A confidence limit for the empiricalmode decomposition and Hilbert spectral analysis," *Proceedings of the Royal Society of London A*, vol. 459, pp. 2317–2345, 2003.

[15] N. E. Huang and Z. Shen, "A new view of nonliner water waves: the Hilbert spectrum," *Annual Review of Fluid Mechanics*, vol. 31, pp. 417–457, 1999.

[16] K. Chen, Y. Li, and L. Chen, "EEMD decomposition in power system fault detection," *Computer Simulation*, vol. 3, pp. 263–266, 2010.

[17] J. S. Cheng, D. Yu, and J. Y. Yang, "A fault diagnosis approach for roller bearings based on EMD method and AR model," *Mechanical Systems and Signal Processing*, vol. 20, no. 2, pp. 350–362, 2006.

[18] J.-Q. E, C.-H. Wang, J. K. Gong et al., "Process on measurement data from copper pyrometallurgical heat dynamical system by using of EMD method," *The Chinese Journal of Nonferrous Metals*, vol. 18, no. 5, pp. 946–951, 2008.

[19] J.-X. Xie, C. T. Cheng, G.-H. Zhou, and Y.-M. Sun, "A new direct multi-step ahead prediction model based on EMD and chaos analysis," *Journal of Automation*, vol. 34, pp. 684–689, 2008.

[20] K. D. Xu, *The Anthology of K. D. Xu-Metallurgical Volume*, Shanghai University Press, Shanghai, China, 2005.

[21] J. Gao, "Asymptotic properties of some estimators for partly linear stationary autoregressive models," *Communications in Statistics—Theory and Methods*, vol. 24, no. 8, pp. 2011–2026, 1995.

[22] H. B. Li, H. Wang, Y. L. Qi, J. H. Hu, and Y. L. Li, "Ilmenite smelted by oxygen-enriched top-blown smelting reduction," *Journal of Iron and Steel Research*, vol. 18, no. 2, pp. 7–13, 2011.

[23] H. H. Fan and L. Y. Zhang, *Statistical Analysis and Application of Eviews*, Mechanical Industry Press, Beijing, China, 2009.